# CLEAR: Calibration-Free Parallel Imaging using Locally Low-Rank Encouraging Reconstruction

Joshua D. Trzasko[1], and Armando Manduca[1]
[1]*Mayo Clinic, Rochester, MN, United States*

**Introduction:** Auto-calibrated parallel imaging (PI) reconstruction strategies are typically formulated such that the target images and system model (e.g., the GRAPPA kernel [1]) are independent variables. These approaches inherently comprise a joint estimation [2-5], corresponding to a challenging bilinear optimization problem in which effort is spent explicitly estimating system models that are nonetheless discarded post-reconstruction. Recently, Lustig et al. [6] proposed a truly "calibration-free" PI (CPI) reconstruction strategy based on exploiting the tendency of the Hankel matrix formed by stacking rasterizations of small k-space blocks to be low-rank. While innovative, this approach has limited scalability – the memory footprint of the constructed Hankel matrix can be well over an order of magnitude larger than that of the target multichannel image set, and performing singular value decompositions (SVD) on such large matrices is computationally challenging. In this work, we propose a novel and efficient image-domain approach to CPI called CLEAR (calibration-free locally low-rank encouraging reconstruction). After reviewing our strategy, we highlight its computational advantages, and demonstrate both its standalone utility and its use in conjunction with sparsity constraints.

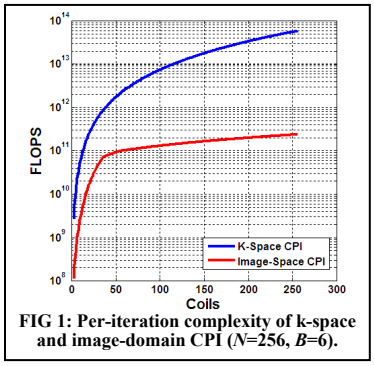

**FIG 1: Per-iteration complexity of k-space and image-domain CPI (*N*=256, *B*=6).**

**Methods:** Without loss of generality, we describe our method for 2D. Suppose we model our acquired signal as $G=AF+n$, where $F$ is a $N^2$x$C$ matrix corresponding to the $C$-channel signal of interest, $A$ is a $N^2 \rightarrow K$ Fourier sampling operator (Cartesian or non-Cartesian), and $n$ is a $K$x$C$ complex Gaussian noise matrix (assumed i.i.d.). Additionally, define $R_b$ as a $B^2$x$N^2$ operator that extracts $B$x$B$ blocks ($B<<N$) from the set of coil images. Note that $F$ can be expressed as $[F](n,c)=[M](n)\cdot[S](n,c)$, where $S$ represents the sensitivity profiles and $M$ is the underlying image. Analogously, $R_bF=\text{diag}(R_bM)R_bS$, In general, $R_bS$ is the rank-determining element. However, since the sensitivity profiles are locally smooth [7], $R_bS$ admits a low-rank decomposition, and $R_bF$ will correspondingly be low-rank. CLEAR exploits this locally low-rank [8] property, and is based on the following optimization problem:

$$\hat{F} = \arg\min_F \left\{ \lambda \sum_{b\in\Omega} \|R_b F\|_* + \|AF - G\|_F^2 \right\} \quad (1)$$

where $\lambda$ is a regularization parameter, and $\|\cdot\|_*$ is the nuclear norm, which is the convex envelope of the rank functional [9]. We define $\Omega$ as the set of all overlapping blocks subject to periodic boundary conditions (translation-invariant). Solutions to (1) can be efficiently generated, e.g., using projected gradient methods – we employ Toh and Yun's [10] matrix generalization of FISTA [11]. Each iteration of this method comprises a first-order update of the objective, and a proximal projection of the penalty which, for (1), is given by:

$$P(X) = B^{-2} \sum_{b\in\Omega} R_b^* S_\lambda(R_b X) \quad (2)$$

where $S_\lambda(\cdot)$ is the singular value soft-thresholding operator [12]. Whereas the k-space CPI approach is based on singular value decomposition (SVD) of a single, large matrix, (2) is based on the SVD of many small matrices. Despite the additional $2C$ Fourier operations in the first-order update, a per-iteration count of floating point operations (FLOPS) [13] reveals that image domain CPI is computationally advantageous, especially in the limit of increasing coils (FIG 1). The memory footprint needed to compute (2) is only on the order of the target image, and so much smaller than that of the k-space approach. We highlight that CLEAR is also very amenable to implementation on modern hardware like GPUs, as collision-free parallelization of (2) can be obtained by noting that $\Omega$ comprises subsets of disjoint blocks. As (1) only exploits properties of the receiver system, for improved reconstruction performance we can also generalize CLEAR to include sparsity penalties. Like low-rankedness, sparsity can be promoted in a block-wise fashion [14], as well as jointly across coils [15], via:

$$\hat{F} = \arg\min_F \left\{ \gamma \sum_{b\in\Omega} \|\Psi R_b F\|_{1,2} + \lambda \sum_{b\in\Omega} \|R_b F\|_* + \|AF - G\|_F^2 \right\} \quad (3)$$

where $\|\cdot\|_{1,2}$ is the $\ell_1$-$\ell_2$ matrix norm, and $\Psi$ is an orthonormal sparsifying transform. (3) can be solved using projections-onto-convex-sets (POCS), variable splitting [16], or by Huang et al.'s [17] recent multi-penalty generalization of FISTA. For the latter method, which we use in this work, the averaged proximal projection associated with (3) is

$$P(X) = B^{-2} \sum_{b\in\Omega} R_b^* \left( \tfrac{1}{2} S_\lambda(R_b X) + \tfrac{1}{2} \Psi^* T_\gamma(\Psi R_b X) \right) \quad (4)$$

where $T_\gamma(\cdot)$ is the joint soft-thresholding operator [15].

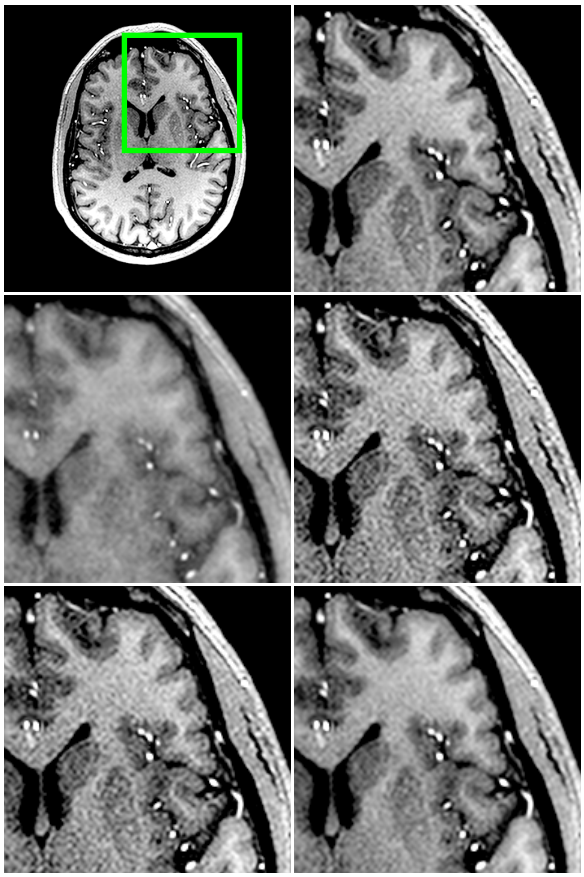
**FIG 2: Enlarged region-of-interests (a) for reconstructions from 3x undersampled 8-channel data: (b) fully-sampled, (c) zero-filling, (d) k-space CPI, (e) CLEAR, (f) CLEAR with block-wise joint sparsity penalty. Coil images were combined via root-sum-of-squares.**

**Results:** FIG 2 shows example reconstructions for one slice of a 3D SPGR data set (FA=20°, TR=15ms, TE=5ms, FOV=24cm, BW=±31.25kHz, N=256) acquired at 1.5T (GE v14.0) with an 8-channel head coil, which was retrospectively 3x undersampled according to a variable-density Poisson disk distribution [15]. Both k-space CPI and CLEAR reconstructions were executed with $B$=8, for 50 iterations. For k-space CPI, 60 (out of 512) singular values were retained during hard thresholding. For CLEAR, two parameter settings, corresponding to without ($\lambda$=40,$\gamma$=0) and with ($\lambda$=20,$\gamma$=10) the sparsity penalty, were evaluated. $\Psi$ was taken as the discrete cosine transform (DCT) [18]. Observe that k-space CPI and CLEAR (only rank penalty) strategies perform similarly in terms of resolution and SNR – the computational advantage of the image-domain approach does not appear to degrade image quality. Due to undersampling, both standalone CPI strategies suffer an unavoidable SNR penalty; however, noise amplification is mitigated by using a sparsity penalty in conjunction with CLEAR.

**Discussion:** We have proposed a novel and efficient image-domain approach to CPI called CLEAR that possesses favorable scalability properties, and readily integrates with sparsity methods. Future directions of investigation include advanced hardware implementations and evaluation for non-Cartesian reconstructions.

**References:** [1] Griswold et al., MRM 2002; [2] Ying et al., MRM 2007; [3] Zhao and Hu, MRM 2008; [4] Uecker et al., MRM 2008; [5] She et al., ISBI 2010 [6] Lustig et al. ISMRM 2010; [7] Pruessmann et al., MRM 1999; [8] Trzasko and Manduca, ISMRM 2011; [9] Recht et al., SIAM Rev 2010; [10] Toh and Yun, Pac J Opt 2010; [11] Beck and Teboulle, SIAM J Img Sci 2009; [12] Cai et al., SIAM J Opt 2010; [13] Golub and Van Loan, Matrix Computations, 3rd Ed.; [14] Baker et al., ISMRM 2009; [15] Lustig et al., ISMRM 2009; [16] Lingala et al., IEEE TMI 2011; [17] Huang et al., Med Img Anal 2011; [18] Guleryuz, IEEE TIP 2007